

Real-Time Scene Graph Generation

Maëlic Neau^{1,2} Paulo E. Santos¹ Karl Sammut¹ Anne-Gwenn Bosser² Cédric Buche^{2,3}
¹College of Science and Engineering, Flinders University, Australia
²Ecole Nationale d'Ingénieurs de Brest, France
³Naval Group Pacific, Australia

{neau, buche, bosser}@enib.fr, {paulo.santos, karl.sammut}@flinders.edu.au

Abstract

Scene Graph Generation (SGG) can extract abstract semantic relations between entities in images as graph representations. This task holds strong promises for other downstream tasks such as the embodied cognition of an autonomous agent. However, to power such applications, SGG needs to solve the gap of real-time latency. In this work, we propose to investigate the bottlenecks of current approaches for real-time constraint applications. Then, we propose a simple yet effective implementation of a real-time SGG approach using YOLOV8 as an object detection backbone. Our implementation is the first to obtain more than 48 FPS for the task with no loss of accuracy, successfully outperforming any other lightweight approaches. Our code is freely available at <https://github.com/Maelic/SGG-Benchmark>.

1. Introduction

Scene Graph Generation (SGG) is the task of generating a structured graph representation from visual inputs. Given an image, visual regions corresponding to objects of interest are extracted, and relations between these objects are predicted in the form of $\langle \textit{subject}, \textit{predicate}, \textit{object} \rangle$ RDF triplets. The connection of these triplets forms a directed acyclic graph which can be interpreted as a structured representation of the scene. In addition, subject and object nodes are traditionally associated with two-dimensional coordinates that account for their respective position on the input image.

During the past few years, this task has attracted a growing interest in the community as a support for other downstream tasks such as Visual Question Answering (VQA) [5], Image Captioning [34], or Reasoning of an embodied agent [7, 17]. However, we observe a significant unbalance between the progress in the SGG task itself and its adoption as a backbone for other downstream tasks. This can be explained by different paradigms but one of them is surely

the lack of simple, low-cost, and effective approaches that could power downstream tasks with low resources or real-time constraints (such as embodied agent reasoning). In this work, we aim to redefine the task of SGG from the perspective of real-time constraints, aiming at bridging the gap between efficient and fast implementations.

Defining the current bottleneck of inference time in SGG is complex, as approaches often rely on the aggregation of diverse modules. These modules are, for the vast majority of approaches, paired as the following pipeline:

1. The object detection module, which predicts candidate bounding box coordinates
2. The features extractor, which associates to each bounding box candidate a feature vector
3. The relation prediction module, which takes as input the bounding boxes and associated features to predict classes, pairs, and relations

In the literature, the (1) object detection and (2) feature extractor modules rely on state-of-the-art approaches such as Faster-RCNN [26] or DETR [2] equipped with a ResNeXt-101 model for feature extraction. To our knowledge, no other feature extractor or bounding box regression module has been used in the task, as approaches are mostly concerned with improving the relation prediction stage considering that the two first stages are independent of the last one. For real-time performance but also overall accuracy, Faster-RCNN, and DETR are today far away from state-of-the-art object detectors such as YOLO (You Only Look Once) [9, 25]. Nonetheless, they are still used because their feature extraction component is deemed better than the ones used in real-time object detectors. However, no quantitative study has been made in this sense specifically for the task of Scene Graph Generation, which is the first aim of this work.

A second aim of this work is to propose a new structure for Scene Graph Generation which is more efficient for real-time processing. In current designs, the workflow

is to sample as many bounding box candidates as possible from the object detection backbone to ease the relation prediction stage. The idea here is that with more bounding boxes as node candidates, more pairs can be created which will facilitate the learning of inter-dependencies between relations. In practice nonetheless, this process is extremely resource-intensive as the complexity of relations prediction grows exponentially with the number of inputs. Another drawback of this method is the decrease in accuracy of the predicted object coordinates and class labels. In fact, as the $\langle \text{subject}, \text{object} \rangle$ pairs are selected based on their potential of having a relation rather than true confidence on the object detection backbone, some nodes from the final graph can be of low confidence from the object detector. On the other hand, some high-confidence objects detected by the object detector can be excluded from the final graph after the relation prediction stage.

In summary, in this work, we successfully leveraged the state-of-the-art real-time object detector YOLOV8 as a feature extraction backbone for the task of SGG and we proposed a new implementation that achieves a competitive runtime latency of 20.5ms with an improved performance of 19.4% in average on a large set of baseline models. Our approach can be easily implemented in any two-stage Scene Graph Generation architecture as we make our code fully open-source and simple to replicate.

2. Related Work

2.1. Scene Graph Generation

Since the first inception of the task [31], SGG has drawn widespread attention in the computer vision and natural language processing communities. Popular approaches combine object detection backbones such as the popular Faster-RCNN [26] with a graph generation model in a two-stage pipeline [14, 19, 28, 29, 31, 38]. However, concerns about biases in large-scale datasets such as Visual Genome [10] have been rapidly raised, resulting in the task of Unbiased SGG [6, 27, 30, 32, 35, 36]. The idea is to improve predicate prediction using different model-agnostic techniques and training strategies such as the Total Direct Effect [27] or probability distribution [15] and evaluate them on a set of baseline models [28, 31, 37]. On the other hand, new approaches [4, 13, 20, 21] are considering the task in a one-stage fashion, learning relationships from image features directly. Even though they are very popular, two-stage approaches are considered to be too complex and unsuited for real-time applications by some [4, 12]. On the other hand, one-stage approaches suffer from low accuracy in object detection and can be challenged to learn complex dependencies in dense scenes [13].

2.2. Real-Time Scene Graph Generation

The term Real-Time Scene Graph Generation has not been widely adopted by the community, unlike Real-Time Object Detection for instance. However, a set of recent approaches are reporting latency metrics in their approach, showing a growing interest in efficient implementations. RelationTransformer (RelTr) [4] and SGTR [13] are two Transformer-based one-stage approaches to the task that report low-latency with 13.4FPS and 6FPS, respectively. Lately, EGTR [8] is a one-stage approach that reports almost state-of-the-art performance with a lower latency of 14.7FPS¹.

While those results are interesting for one-stage approaches, the real-time performance of two-stage approaches has not been studied yet. At the same time, the link between the performance of the object detector and the performance of models on the task is unclear, as different approaches use different backbones with different settings but yet compare their results together. In this work, we aim to bridge this gap by proposing the first true real-time (i.e. inference > 30 FPS) implementation of SGG while improving overall accuracy. We also study the main parameters that influence latency for Scene Graph Generation.

3. Approach

3.1. Features Extraction Backbone

We modify different SGG architectures originally based on Faster-RCNN to evaluate the performance of YOLOV8 as a feature extractor. In previous work, Faster-RCNN is equipped with a ResNeXt-101 backbone with an output channel size of 256. YOLOV8 is equipped with a CSPDarknet53 backbone with a channel size of 192. We modify the forward pass of YOLOV8 to extract features from the backbone before the classification and regression heads, which correspond to the last layers of what we call the neck in Yolo’s style architectures. YOLOV8 architecture is slightly different here from Faster-RCNN as it processes features at three fixed scales, to better detect small, medium, and large size objects. From the inner representation of the network, this corresponds to layers 15, 18, and 21 respectively. To cope with this issue, we then modify the original ROI Align algorithm of Faster-RCNN to assign to each of the three feature maps extracted from the three layers the corresponding proposals, based on every bounding box area size. Then, ROI Align is performed as in the original implementation.

Next, we tried to understand the impact of those changes in the relation prediction stage. To do so, we trained different relation prediction models by keeping both backbones frozen. During training and evaluation, we purposely input ground truth bounding boxes and pairs to evaluate only the

¹Inference time reported in [8] using one NVIDIA V100.

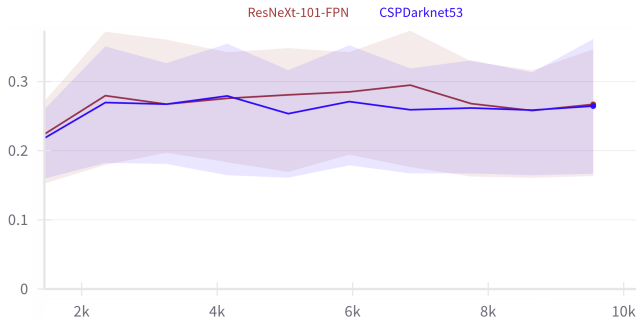


Figure 1. Performance in F1@K for relation prediction of different models [27, 28, 37] equipped with Faster-RCNN and YOLOV8 backbones.

prediction of relations. This type of evaluation is known as predicate classification (PredCls). In Fig. 1 we display a comparison of the performance of three different baseline models, Motifs-TDE [27], VCTree-TDE [27] and Transformer [27] equipped with the feature extractor of YoloV8 (CSPDarknet53) and Faster-RCNN (ResNeXt-101). For each model, the metric used is F1@K which is the harmonic average between the commonly used metric Recall@K, and meanRecall@K. We observed almost no difference between the two, which can signify that either the visual features are not important in the learning process of relation prediction or that the quality of the features generated by the YoloV8 backbone and Faster-RCNN ones are very similar. This is an interesting finding, as the size and architecture of both backbones are very different.

3.2. Object Classification

The traditional approach in object detection employs a bounding box regression and a classification head after the feature extraction step. In the original Faster-RCNN implementation, regression and classification are done in a sequence, and then a final step of Non-Maximum Suppression (NMS) is applied.

In the case of the two-stage approach in SGG with a Faster-RCNN backbone, the strategy employed is to decode object classes during the relation prediction stage, to better capture object co-occurrences. While in the original Faster-RCNN implementation a simple softmax is applied to the class logits, SGG approaches are introducing their own method to decode classes, for instance a TreeLSTM for VCTree [28]. This makes the performance of SGG models to be different than the original Faster-RCNN implementation. This can also lead to severe biases in the comparison of models in the task of Scene Graph Generation, as the difference in performance for object detection may hinder the comparison of relation prediction modules.

On top of that, in SGG mode the step of NMS is performed after the relation prediction stage which will also

Backbone	Relation Head	mAP@50	mAP@50-95
Faster-RCNN	-	27.2	11.5
	Motifs-TDE [27]	26.2	11.6
	VC-Tree [28]	25.5	11.1
	PE-NET [39]	25.2	11.2
	Transformer [27]	24.2	10.6
	GPS-NET [19]	17.4	7.1
YOLOV8	[19, 27, 39]	35.1	20.0

Table 1. Performance on Object Detection of Faster-RCNN before and after the Relation Prediction stage with different SGG models on the Visual Genome dataset [10].

influence the predicted objects. As a result, the performance of SGG models in object detection becomes slightly worse after the relation training stage than before. We draw a comparison of the performance of the Faster-RCNN model trained on the Visual Genome dataset with different relation prediction heads, on the same validation set in Tab. 1. In this table, we can see that the performance in object detection drops significantly, from 1% for Motifs-TDE to almost 10% in mAP@50 for GPS-NET. These results show a true dependence between the two stages of SGG methods, in contrast to what is usually accepted in the community.

To solve this problem, we propose to completely make independent the first and second stages of the Scene Graph Generation process. To do so, we freeze the regression but also the classification head of YOLOV8 and perform NMS before the relation prediction stage. The objective of the relation prediction stage becomes then to predict only the pairs and associate predicates, in contrast to also predicting the class labels of objects. This significantly lowers the complexity of the relation prediction stage and thus the computational load of the model. With this method, our performance in mAP stays similar after any relation prediction training, which also helps to fairly evaluate the quality of relation predicted by Scene Graph Generation models.

3.3. Candidate Selection

During the step of relation prediction, all proposals are considered valid node candidates for the graph refinement process. Traditionally, a fixed number of proposals (i.e. 80 proposals) is considered from the higher confidence proposals output by the object detector. The idea here is that by sampling a large number of proposals, it is easier to find valid pairs and relations. However, this results in considerably enlarging the number of computations required to generate a good graph, which is a bottleneck for real-time applications. This issue also raises concerns about the objective of the task, as it could be considered unfair to look for candidate nodes of the graph based on their likelihood of having a relation rather than the true confidence of the object detector. For instance, a low-confidence bounding box `chair` (which could be ranked bottom 80 in the detected

proposals) could be selected as a node candidate instead of a higher-confidence bounding box `kite` if the two objects are in the presence of a third one, `table`, as `chair` is more likely to have a relation with `table` than `kite`. This paradigm will tend to improve the performance of models for relation prediction but with the drawback of lowering the accuracy in object detection and limiting the generalization to new or unseen relations. The question here is: *do we want models to predict relations from a small set of highly confident objects in the scene or do we want models to predict the most likely relations from a larger set of objects, even though some of those objects are of low confidence?*

In this work, we believe the first approach is more beneficial for real-time applications. We hypothesize that the gain in latency is more important than the gain in accuracy by using a small number of proposals, such as 10 or 20 per image and that an optimal trade-off can be found. For the relation prediction stage, as we are evaluating entire triplets and not solely the predicate, the relation triplets score is computed with the following formula:

$$\theta_{rel} = \theta_{obj} * \theta_{pred} * \theta_{subj} \quad (1)$$

With θ_{pred} being the confidence score of a predicate given $\langle subject, object \rangle$ pair as candidate and $\theta_{obj}, \theta_{subj}$ are the respective confidence score of the object detector. This formula gives more weight to the confidence of the subject and object than the predicate, which makes the model’s overall performance rely more on the object detector than the relation predictor. Thus, one would rather want to input only highly confident proposals to the relation prediction stage. We evaluate this hypothesis in the next sections.

4. Metrics

During the years, the SGG task has seen many metrics being proposed such as Recall@K, meanRecall@K, or F1@K. All these metrics are used to validate the performance of models, with different goals. MeanRecall@K is targeted into the performance on rare and tail classes and F1@K is the harmonic average between overall performance and tail classes performance. @K means that we compute the recall on the top k relations predicted after the final stage of an SGG model. The mR@K and R@K metrics have been criticized a lot for being metrics that could be easily cheated on. For instance, a simple model with no visual features and only statistical biases about objects and predicates co-occurrence in the dataset can attain a high mR@K and R@K, even outperforming a lot of approaches that use visual features [16]. This is for sure not what we want to benchmark SGG models for real-world applications. To cope with this issue, we propose to use a new metric, the Informative Recall @K (IR@K) which asserts the quality of generated scene graphs by comparing them with relations contained in corresponding scene

descriptions (i.e. detailed image captions). As the scene descriptions are only used for evaluation, it is impossible to tweak the model using frequency bias to boost the performance artificially. To retrieve good-quality captions for the Visual Genome dataset [10], we used annotated image descriptions from the COCO-captions [3] which intersect for more than 50% with VG. Captions for the rest of the images were generated using the state-of-the-art BLIP-2 model [11] for image captioning, which is pre-trained on COCO-captions. Given the captions, we generated Textual Scene Graphs using the Stanford NLP Parser, following the SPICE method [1]. Here the idea is to use several parsing rules to extract $\langle subject, predicate, object \rangle$ triplets from the free-form caption. Finally, we computed the cosine similarity distance ($\theta = 0.9$) between GLoVe language embeddings [24] of triplets from the generated Scene Graphs and the Textual Scene Graph (TSG) associated with the same image, as the vocabulary of the two distributions is different. We kept only the top-1 distance for every triplet in the VSG as a match with the corresponding TSG triplet and aggregated all results per image, as in original R@k and mR@k implementations.

5. Experiments

In the following, we compare the performance in latency and accuracy metrics between traditional two-stage approaches with Faster-RCNN equipped with a ResNeXt-101 and our new architecture which uses YOLOV8 exclusively as an object detection backbone. In SGG, the most widely used dataset is Visual Genome [10]. The commonly used split of the data is called VG150 and contains annotations from the top 150 object classes and top 50 predicate classes. However, this split of the data suffers from severe biases [23, 33] and issues such as the presence of ambiguous classes (e.g. the classes "people", "men" etc) [18, 33]. To cope with this problem, we decided to use the IndoorVG split of the dataset, which is a smaller version with 83 object classes and 37 predicate classes. This split has been manually curated to remove wrong or ambiguous classes [22].

Regarding our object detector, YOLOV8 comes in different variants, ranging from nano to large. For the following experiments, we use the medium version, YOLOV8m. Our YOLOV8 model has been trained for 100 epochs on the Visual Genome dataset with a batch size of 16, following the official implementation ².

5.1. Comparison with two-stage approaches

We experimented our approach for five different relation prediction models: Motifs-TDE [27, 37], VCTree-TDE [27, 28], Transformer [27], GPS-Net [19] and PENET [39]. We computed the standard Recall@k metric for

²<https://github.com/ultralytics/ultralytics>

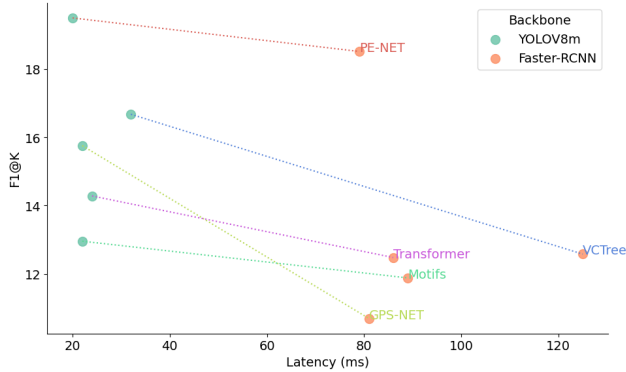


Figure 2. Latency versus F1@k for different models equipped with the Faster-RCNN backbone and our modified YOLOV8 backbone.

$k = [20, 50, 100]$ and meanRecall@k for $k = [20, 50, 100]$. Both metrics for all settings of k are averaged in the F1@k metric, which efficiently represents the trade-off for the model performance between head and tail predictions. For all approaches, we re-trained the standard implementation by authors with both the Faster-RCNN backbone and our modified YOLOV8 backbone. For all tests, we benchmark latency on one Nvidia A6000 GPU with batch size 1 and image size 640*640. The latency reported is the combination of object detection and relation prediction stages for all models.

In Fig. 2 we display the difference in latency and F1@k for the five different models. Using YOLOV8, we experienced an average improvement of 19.4% in F1@k compared to Faster-RCNN. This improvement is obviously due to the overall gain of the accuracy of YOLOV8m in object detection, which performs at 35.1 mAP@50 versus 27.2 for Faster-RCNN on the Visual Genome dataset, see Tab. 1. However, the gain in F1@k is not very strongly correlated to the gain in mAP@50, as we measure a Pearson correlation coefficient of 0.80 between the two gains. Regarding latency, we demonstrate an average improvement of 2.75x for using YOLOV8 instead of Faster-RCNN, which is a considerable gap. The difference in latency between the five models tested is also lower with YOLOV8 than Faster-RCNN, this is due to the step of object classification which has been removed in our implementation. As relation heads do not need to compute object classes, computational complexity becomes lower and their average execution time for relation prediction becomes very similar. The best model in F1@K, PE-NET [39], is also the fastest one with a latency of 20.5ms which is a good choice for real-time constraints. Under those settings, an average of 48FPS can be attained, which is significantly higher than any other reported value in the past for the task.

As said earlier, the meanRecall@k and Recall@k metrics can be easily cheated on and do not efficiently repre-

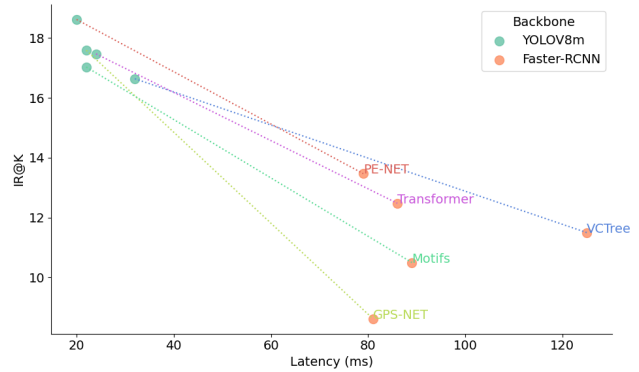


Figure 3. Latency versus IR@k for different models equipped with the Faster-RCNN backbone and our modified YOLOV8 backbone.

sent the performance of a model to produce useful graphs for real-world applications, mainly because it does not take into account the importance weight of relations to describe the scene. We used the introduced IR@k metric with $k = [5, 10]$ to evaluate this last point. Here we purposely choose low values of k as the main goal of this metric is to represent the ability of models to output informative predictions with confidence, such that top predictions can be directly sampled for reasoning. We assume that in real-world applications a small number of high-quality relations is more beneficial than a high number of medium to low-quality relations to describe a scene.

We compare our approach with YOLOV8m and traditional Faster-RCNN in Fig. 3, the metric reported is the average of IR@5 and IR@10. Surprisingly, we observe a net improvement using YOLOV8 for all models. In contrast to F1@k, performance is very close for all models, which highlights the importance of proposal quality to produce informative scene graphs.

5.2. Latency and Number of Proposals

In the following, we dive into the principal variable responsible for latency gain in Scene Graph Generation: the number of proposals. As explained before, the second stage of SGG takes as input a fixed number of n proposals as node candidates and finds correct pairs and predicates. There could be a maximum of $n * (n - 1)$ possible pairs in the graph, thus when doing matching the computational complexity is supposed to scale accordingly. To demonstrate this hypothesis, we evaluate the performance of the PE-NET model [39] in both latency and accuracy for different numbers of input proposals, ranging from 10 to 150 per image, with a step of 10. For all experiments, we ranked proposals by confidence of the backbone and selected the top ones. For YOLOV8, proposals are ranked after NMS.

We display the results of those experiments in Fig. 4. Interestingly, we observe a plateau phenomenon using

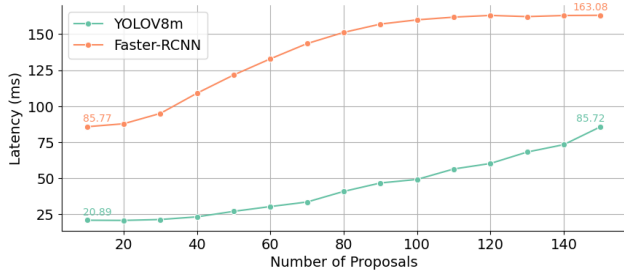


Figure 4. Latency for the PE-NET model [39] using different number of proposals per image, with batch size = 1.

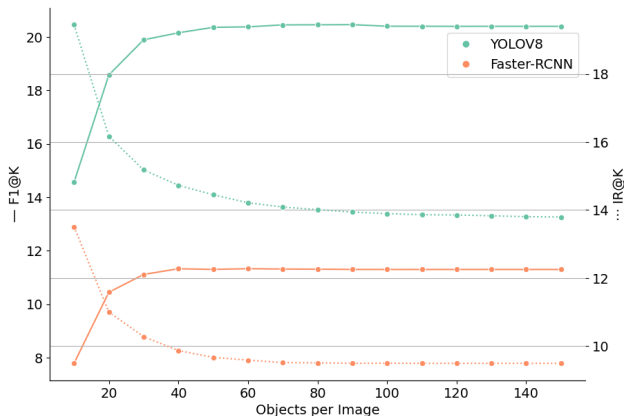


Figure 5. Average F1@k and IR@k performance for the PE-NET model [39] using a different number of proposals per image, with batch size 1.

the Faster-RCNN above 100 proposals, which doesn't appear when using YOLOV8. By using 150 proposals with YOLOV8, the latency is similar to 10 proposals with Faster-RCNN. To find the best trade-off between latency and performance, we also measured the average F1@k for different numbers of proposals, see Fig. 5. In this figure, we can see that for both models, an optimal F1@k (left axis, plane line) is obtained at around 40 proposals per image. This means that the top 40 proposals returned by YOLO or Faster-RCNN are of good enough quality to be valid node candidates for the graph refinement step. In the same plot, we also measure the average IR@k for the same set of settings (right axis, dotted line). Interestingly, we observe a high IR@k for the lowest number of proposals, 10, even if the average F1@k is not maximal. These results confirm the assumption that to obtain informative graphs, the quality of object proposals is of utmost importance. By crossing those numbers with latency per number of proposals (see Fig. 4), we can find an optimal implementation for F1@k with $n = 40$ and $n = 18$ for an optimal F1@k to IR@k trade-off for both YOLOV8 and Faster-RCNN.

6. Conclusion

In this work, we propose the first implementation of a true real-time Scene Graph Generation procedure by leveraging the YOLOV8 object detector, with an average improvement of 19.4% in the F1@k metric for the task. Our main finding is that the performance and latency of SGG models are heavily correlated with the quality and quantity of object proposals generated by the object detector. However, regarding both overall performance and latency, an optimal trade-off can be found by using 40 object proposals as input to the relation prediction stage. We also share findings on the quality of generated graphs related to the amount of informative relations they contain. In contrast to standard evaluation metrics that measure the correctness of relations prediction, we propose a new metric, the InformativeRecall@k (IR@k), which efficiently benchmarks the ability of models to produce informative relations first. Using this metric, we observed that a low number (i.e. 10) of high-quality proposals produces a more informative graph even though relations for this number of proposals are deemed of less quality by standard metrics. This last point illustrates the limits and challenges of current evaluation metrics and benchmarks used in the task which may not be appropriate to evaluate real-world use cases of Scene Graph Generation.

References

- [1] Peter Anderson, Basura Fernando, Mark Johnson, and Stephen Gould. Spice: Semantic propositional image caption evaluation. In *Computer Vision—ECCV 2016: 14th European Conference, Amsterdam, The Netherlands, October 11–14, 2016, Proceedings, Part V 14*, pages 382–398. Springer, 2016. 4
- [2] Nicolas Carion, Francisco Massa, Gabriel Synnaeve, Nicolas Usunier, Alexander Kirillov, and Sergey Zagoruyko. End-to-end object detection with transformers. In *European conference on computer vision*, pages 213–229. Springer, 2020. 1
- [3] Xinlei Chen, Hao Fang, Tsung-Yi Lin, Ramakrishna Vedantam, Saurabh Gupta, Piotr Dollár, and C Lawrence Zitnick. Microsoft coco captions: Data collection and evaluation server. *arXiv preprint arXiv:1504.00325*, 2015. 4
- [4] Yuren Cong, Michael Ying Yang, and Bodo Rosenhahn. ReLTR: Relation Transformer for Scene Graph Generation, Aug. 2022. arXiv:2201.11460 [cs] version: 2. 2
- [5] Vinay Damodaran, Sharanya Chakravarthy, Akshay Kumar, Anjana Umashy, Teruko Mitamura, Yuta Nakashima, Noa Garcia, and Chenhui Chu. Understanding the role of scene graphs in visual question answering. *arXiv preprint arXiv:2101.05479*, 2021. 1
- [6] Xingning Dong, Tian Gan, Xuemeng Song, Jianlong Wu, Yuan Cheng, and Liqiang Nie. Stacked Hybrid-Attention and Group Collaborative Learning for Unbiased Scene Graph Generation. In *2022 IEEE/CVF Conference on Computer Vision and Pattern Recognition (CVPR)*, pages 19405–19414, New Orleans, LA, USA, June 2022. IEEE. 2

- [7] Samir Yitzhak Gadre, Kiana Ehsani, Shuran Song, and Roozbeh Mottaghi. Continuous scene representations for embodied ai. In *Proceedings of the IEEE/CVF Conference on Computer Vision and Pattern Recognition*, pages 14849–14859, 2022. 1
- [8] Jinbae Im, JeongYeon Nam, Nokyoung Park, Hyungmin Lee, and Seunghyun Park. Egtr: Extracting graph from transformer for scene graph generation. *arXiv preprint arXiv:2404.02072*, 2024. 2
- [9] Glenn Jocher, Ayush Chaurasia, and Jing Qiu. Ultralytics YOLO, Jan. 2023. 1
- [10] Ranjay Krishna, Yuke Zhu, Oliver Groth, Justin Johnson, Kenji Hata, Joshua Kravitz, Stephanie Chen, Yannis Kalantidis, Li-Jia Li, David A. Shamma, Michael S. Bernstein, and Li Fei-Fei. Visual Genome: Connecting Language and Vision Using Crowdsourced Dense Image Annotations. *International Journal of Computer Vision*, 123(1):32–73, May 2017. 2, 3, 4
- [11] Junnan Li, Dongxu Li, Silvio Savarese, and Steven Hoi. Blip-2: Bootstrapping language-image pre-training with frozen image encoders and large language models. In *International conference on machine learning*, pages 19730–19742. PMLR, 2023. 4
- [12] Lin Li, Long Chen, Yifeng Huang, Zhimeng Zhang, Songyang Zhang, and Jun Xiao. The Devil is in the Labels: Noisy Label Correction for Robust Scene Graph Generation. In *2022 IEEE/CVF Conference on Computer Vision and Pattern Recognition (CVPR)*, pages 18847–18856, New Orleans, LA, USA, June 2022. IEEE. 2
- [13] Rongjie Li, Songyang Zhang, and Xuming He. SGTR: End-to-end Scene Graph Generation with Transformer. In *2022 IEEE/CVF Conference on Computer Vision and Pattern Recognition (CVPR)*, pages 19464–19474, New Orleans, LA, USA, June 2022. IEEE. 2
- [14] Rongjie Li, Songyang Zhang, Bo Wan, and Xuming He. Bipartite Graph Network with Adaptive Message Passing for Unbiased Scene Graph Generation. In *2021 IEEE/CVF Conference on Computer Vision and Pattern Recognition (CVPR)*, pages 11104–11114, Nashville, TN, USA, June 2021. IEEE. 2
- [15] Wei Li, Haiwei Zhang, Qijie Bai, Guoqing Zhao, Ning Jiang, and Xiaojie Yuan. PDDL: Predicate Probability Distribution based Loss for Unbiased Scene Graph Generation. In *2022 IEEE/CVF Conference on Computer Vision and Pattern Recognition (CVPR)*, pages 19425–19434, New Orleans, LA, USA, June 2022. IEEE. 2
- [16] Xingchen Li, Long Chen, Jian Shao, Shaoning Xiao, Songyang Zhang, and Jun Xiao. Rethinking the Evaluation of Unbiased Scene Graph Generation, Oct. 2022. arXiv:2208.01909 [cs]. 4
- [17] Xinghang Li, Di Guo, Huaping Liu, and Fuchun Sun. Embodied semantic scene graph generation. In *Conference on robot learning*, pages 1585–1594. PMLR, 2022. 1
- [18] Yuanzhi Liang, Yalong Bai, Wei Zhang, Xueming Qian, Li Zhu, and Tao Mei. VrR-VG: Refocusing Visually-Relevant Relationships. In *2019 IEEE/CVF International Conference on Computer Vision (ICCV)*, pages 10402–10411, Seoul, Korea (South), Oct. 2019. IEEE. 4
- [19] Xin Lin, Changxing Ding, Jinquan Zeng, and Dacheng Tao. GPS-Net: Graph Property Sensing Network for Scene Graph Generation. In *2020 IEEE/CVF Conference on Computer Vision and Pattern Recognition (CVPR)*, pages 3743–3752, Seattle, WA, USA, June 2020. IEEE. 2, 3, 4
- [20] Si Liu, Zitian Wang, Yulu Gao, Lejian Ren, Yue Liao, Guanghui Ren, Bo Li, and Shuicheng Yan. Human-centric Relation Segmentation: Dataset and Solution. *IEEE Transactions on Pattern Analysis and Machine Intelligence*, pages 1–1, 2021. Conference Name: IEEE Transactions on Pattern Analysis and Machine Intelligence. 2
- [21] Yichao Lu, Himanshu Rai, Jason Chang, Boris Knyazev, Guangwei Yu, Shashank Shekhar, Graham W. Taylor, and Maksims Volkovs. Context-aware Scene Graph Generation with Seq2Seq Transformers. In *2021 IEEE/CVF International Conference on Computer Vision (ICCV)*, pages 15911–15921, Montreal, QC, Canada, Oct. 2021. IEEE. 2
- [22] Maëlic Neau, Paulo Santos, Anne-Gwenn Bosser, and Cédric Buche. In defense of scene graph generation for human-robot open-ended interaction in service robotics. In *Robot World Cup*, pages 299–310. Springer, 2023. 4
- [23] Maëlic Neau, Paulo E Santos, Anne-Gwenn Bosser, and Cédric Buche. Fine-grained is too coarse: A novel data-centric approach for efficient scene graph generation. In *Proceedings of the IEEE/CVF International Conference on Computer Vision*, pages 11–20, 2023. 4
- [24] Jeffrey Pennington, Richard Socher, and Christopher D Manning. Glove: Global vectors for word representation. In *Proceedings of the 2014 conference on empirical methods in natural language processing (EMNLP)*, pages 1532–1543, 2014. 4
- [25] Joseph Redmon, Santosh Divvala, Ross Girshick, and Ali Farhadi. You only look once: Unified, real-time object detection. In *Proceedings of the IEEE conference on computer vision and pattern recognition*, pages 779–788, 2016. 1
- [26] Shaoqing Ren, Kaiming He, Ross Girshick, and Jian Sun. Faster r-cnn: Towards real-time object detection with region proposal networks. *Advances in neural information processing systems*, 28, 2015. 1, 2
- [27] Kaihua Tang, Yulei Niu, Jianqiang Huang, Jiaxin Shi, and Hanwang Zhang. Unbiased Scene Graph Generation From Biased Training. In *2020 IEEE/CVF Conference on Computer Vision and Pattern Recognition (CVPR)*, pages 3713–3722, Seattle, WA, USA, June 2020. IEEE. 2, 3, 4
- [28] Kaihua Tang, Hanwang Zhang, Baoyuan Wu, Wenhan Luo, and Wei Liu. Learning to Compose Dynamic Tree Structures for Visual Contexts. In *2019 IEEE/CVF Conference on Computer Vision and Pattern Recognition (CVPR)*, pages 6612–6621, Long Beach, CA, USA, June 2019. IEEE. 2, 3, 4
- [29] Wenbin Wang, Ruiping Wang, Shiguang Shan, and Xilin Chen. Exploring Context and Visual Pattern of Relationship for Scene Graph Generation. In *2019 IEEE/CVF Conference on Computer Vision and Pattern Recognition (CVPR)*, pages 8180–8189, Long Beach, CA, USA, June 2019. IEEE. 2
- [30] Bin Wen, Jie Luo, Xianglong Liu, and Lei Huang. Unbiased Scene Graph Generation via Rich and Fair Semantic Extraction, Feb. 2020. arXiv:2002.00176 [cs]. 2

- [31] Danfei Xu, Yuke Zhu, Christopher B. Choy, and Li Fei-Fei. Scene Graph Generation by Iterative Message Passing. In *Proceedings of the IEEE Conference on Computer Vision and Pattern Recognition*, pages 5410–5419, 2017. 2
- [32] Shaotian Yan, Chen Shen, Zhongming Jin, Jianqiang Huang, Rongxin Jiang, Yaowu Chen, and Xian-Sheng Hua. PCPL: Predicate-Correlation Perception Learning for Unbiased Scene Graph Generation. In *Proceedings of the 28th ACM International Conference on Multimedia*, pages 265–273, Seattle WA USA, Oct. 2020. ACM. 2
- [33] Jingkang Yang, Yi Zhe Ang, Zujin Guo, Kaiyang Zhou, Wayne Zhang, and Ziwei Liu. Panoptic Scene Graph Generation. In Shai Avidan, Gabriel Brostow, Moustapha Cissé, Giovanni Maria Farinella, and Tal Hassner, editors, *Computer Vision – ECCV 2022*, Lecture Notes in Computer Science, pages 178–196, Cham, 2022. Springer Nature Switzerland. 4
- [34] Xuewen Yang, Yingru Liu, and Xin Wang. Reformer: The relational transformer for image captioning. In *Proceedings of the 30th ACM International Conference on Multimedia*, pages 5398–5406, 2022. 1
- [35] Kanghoon Yoon, Kibum Kim, Jinyoung Moon, and Chanyoung Park. Unbiased Heterogeneous Scene Graph Generation with Relation-aware Message Passing Neural Network, Dec. 2022. arXiv:2212.00443 [cs] version: 1. 2
- [36] Jing Yu, Yuan Chai, Yujing Wang, Yue Hu, and Qi Wu. CogTree: Cognition Tree Loss for Unbiased Scene Graph Generation. In *Proceedings of the Thirtieth International Joint Conference on Artificial Intelligence*, pages 1274–1280, Montreal, Canada, Aug. 2021. International Joint Conferences on Artificial Intelligence Organization. 2
- [37] Rowan Zellers, Mark Yatskar, Sam Thomson, and Yejin Choi. Neural Motifs: Scene Graph Parsing with Global Context. In *2018 IEEE/CVF Conference on Computer Vision and Pattern Recognition*, pages 5831–5840, Salt Lake City, UT, June 2018. IEEE. 2, 3, 4
- [38] Hanwang Zhang, Zawlin Kyaw, Shih-Fu Chang, and Tat-Seng Chua. Visual Translation Embedding Network for Visual Relation Detection. In *2017 IEEE Conference on Computer Vision and Pattern Recognition (CVPR)*, pages 3107–3115, Honolulu, HI, July 2017. IEEE. 2
- [39] Chaofan Zheng, Xinyu Lyu, Lianli Gao, Bo Dai, and Jingkuan Song. Prototype-based embedding network for scene graph generation. In *Proceedings of the IEEE/CVF Conference on Computer Vision and Pattern Recognition*, pages 22783–22792, 2023. 3, 4, 5, 6